Hindawi
Geofluids
Volume 2022, Article ID 5304250, 11 pages
https://doi.org/10.1155/2022/5304250

Research Article

Analysis of Energy Transmission and Deformation Characteristics of Coal-Rock Combined Bodies

Wang Tuo[1,2] **Qi Fuzhou**[3] **and Chang Jucai**[1,2]

[1]*State Key Laboratory of Mining Response and Disaster Prevention and Control in Deep Coal Mines, Anhui University of Science and Technology, Huainan, Anhui, China 232001*
[2]*Open Research Grant of Joint National-Local Engineering Research Centre for Safe and Precise Coal Mining, Anhui University of Science and Technology, Huainan, Anhui, China 232001*
[3]*School of Civil and Architecture Engineering, Zhongyuan University of Technology, Zhengzhou, Henan, China 450007*

Correspondence should be addressed to Chang Jucai; jcchang@aust.edu.cn

Received 24 April 2022; Revised 17 May 2022; Accepted 30 May 2022; Published 28 June 2022

Academic Editor: Yingfeng Sun

A coal-rock system is a common combination form in coal mines. In order to explore the energy interchange law of a coal-rock combined body and the interaction relationship between the two bodies, loading tests of coal-rock combined bodies with different height ratios were carried out. The loading path of rock in coal-rock combined bodies was demonstrated by means of a single loading and unloading test of the same-sized rock sample. Furthermore, a method to calculate rock energy was proposed based on the area of the loading and unloading curve. The experimental results show that the greater the surrounding rock pressure is, the smaller increase rate of lateral and volumetric strain in the postpeak stage will be when the same height ratio is present. An increase in the surrounding rock pressure causes an increase in the total strain energy density of small-sized rock samples. However, the total strain energy density is always greater than the elastic strain energy density. And the elastic and dissipated strain energy densities also increase, along with the energy dissipation with unloading. When the proportion of coal bodies increases, the energy accumulation also shows an increasing trend. When the height of the coal is greater than half the height of the complete specimen, the coal energy proportion is greater than 60%. After reaching the yield load, the energy in the coal body is dissipated in forms such as plastic deformation, internal damage, block friction, radiation energy, and kinetic energy. Therefore, the energy released is, in part, reflected in the rock body.

1. Introduction

Energy transformation is the essential characteristic of various physical changes and the cause of the damage and destruction of rocks. The energy transformation of a rock load-carrying process is dynamic and includes an input, accumulation, dissipation, and release of energy, as well as the evolution of microcracks to macrocracks inside the rock [1–10]. Studying the deformation and failure laws of coal-rock combined bodies from the perspective of energy is closer to its failure essence, enriching and deepening people's understanding of the mechanical behavior of loaded coal-rock combined bodies. Many experts and scholars have studied the process of energy transformation in rock loading. Cook [11] first studied rock stability and the energy released by rock damage per unit volume. Gao et al. [12] studied the energy evolution in the process of rock deformation and destruction, and the results showed that the energy evolution curve was clearly phased, and the probability of rock explosion was also analyzed according to the energy conservation index. Gong et al. [13, 14] proposed a formula for storing peak strength strain energy considering the rockburst tendency and analyzed the elasticity and dissipative strain energy density in the rock loading process. Meng et al. [15] studied the evolution and distribution of rock energy under triaxial cyclic loading and unloading conditions. Tu et al. [16] studied the stress conditions for the failure or crushing of intact coal and estimated the minimum stress for an intact coal outburst. Meanwhile, He et al. [17, 18] studied the relationship between the rockburst rating

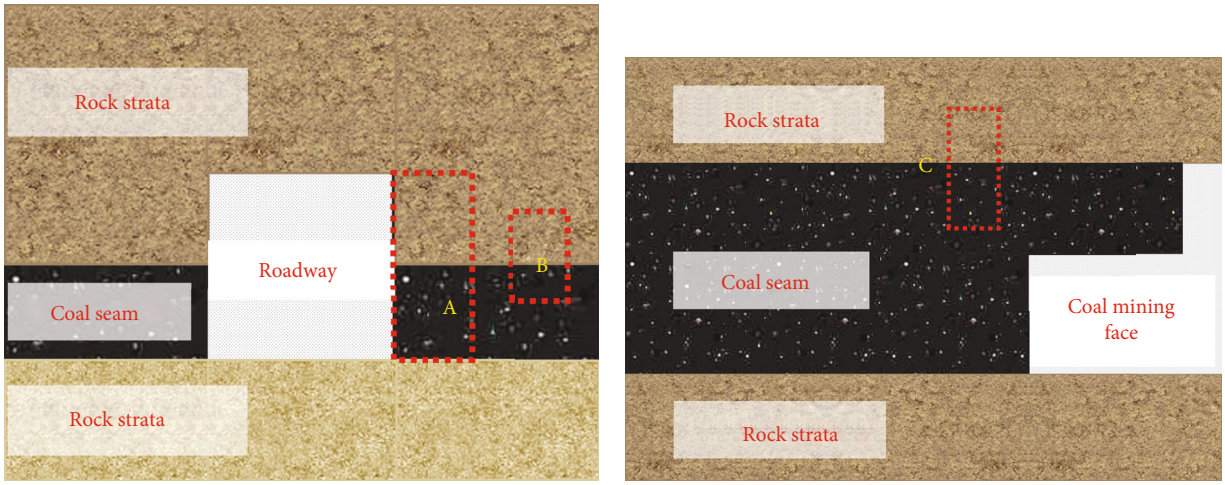

(a) (b)

Figure 1: A common form of coal-rock combined body in coal mines. (a) Half-coal-rock laneway. (b) Working surface.

and the radius of the plastic zone and radial stress and proposed a new rockburst criterion to predict the rockburst classification.

Furthermore, many scholars have conducted experimental research on the mechanical behavior of coal-rock systems, including uniaxial compression tests, triaxial compression tests, and split Hopkinson pressure bar dynamic tests [19–22]. Some scholars have also studied the deformation and destruction law, acoustic emission, and burst tendency characteristics in the loading process of coal-rock combined systems [23–32]. Xiao et al. [33] studied the relationship between the dynamic properties of combined coal-rock and acoustic emission-charge signals and gave the signal identification methods of different burst tendency specimens. Dou et al. [34] studied the electromagnetic radiation law of the impact destruction of coal-rock combined bodies and showed experimentally that electromagnetic radiation signals could predict the destruction of a coal-rock system. Liu et al. [35] studied the acoustic emission characteristics and rockburst tendencies of coal-rock combined bodies through numerical simulation tests. Zhang [36] studied the precursor information of coal-rock destruction using infrared thermal imaging and acoustic emission. The effects of water and temperature on the mechanics of coal-rock combined body at different height ratios have been studied by other scholars [37–40]. Presently, the study of the energy evolution law of a single rock has become more mature; however, relying on the energy evolution law of a single rock cannot reflect the phenomenon of cracking-through or rupture of a coal-rock formation system. Furthermore, the energy transfer law of coal-rock combined systems at different combination heights has rarely been reported on.

Coal-rock systems are a common rock combination form in coal mine sites. The lower strength block determines the peak strength of coal-rock combined bodies. Rocks and coals of different heights have different strengths; thus, the energy accumulated and released also varies (when destruction conditions are met). This paper studies the uniaxial and

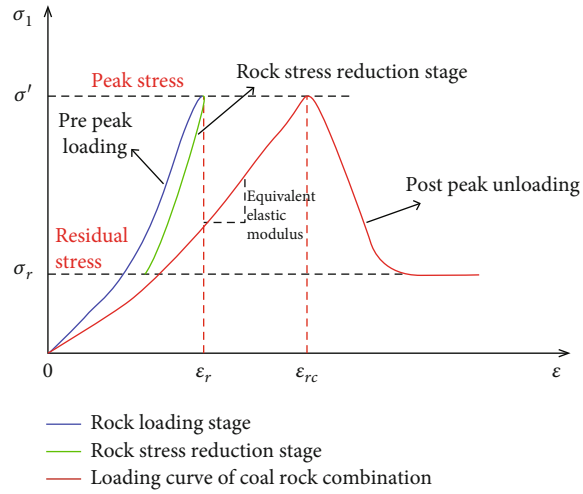

Figure 2: Stress-strain relationship of rock and coal-rock combined body during loading.

conventional triaxial compression tests of coal-rock combined systems with different height ratios. The research on the storage, dissipation characteristics, and energy conversion laws of the internal energy of coal and rock bodies in the loading process are of great help to understand the interaction and function of various rock strata in the field construction and play a guiding role in proposing the pressure relief in the key layer of energy accumulation and releasing energy and alleviating the risk of rockburst of great significance in solving the deformation and burst tendency analysis of surrounding field rock system, which also brings new perspectives and solutions to relevant rock engineering practices.

2. Test Process

In mining engineering, the surrounding rock pressure increases from the surface of the roadway to the interior of the surrounding rock mass, and the coal-rock combined

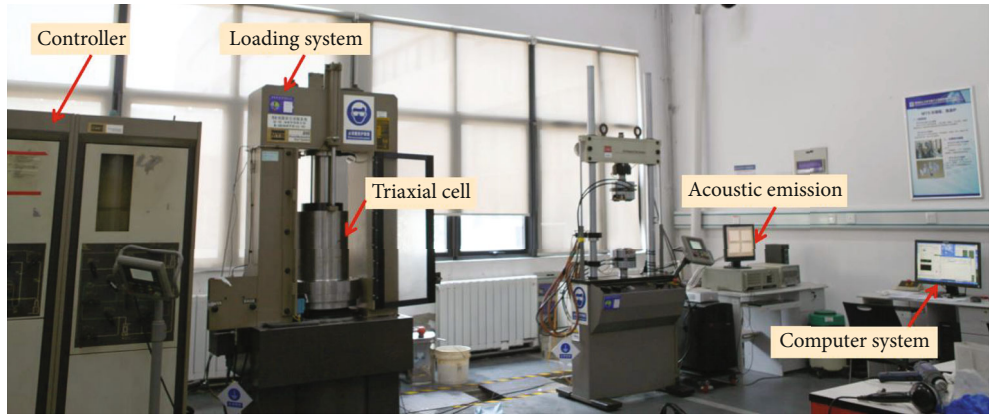

Figure 3: MTS815.02 electroliquid servo rock mechanics test equipment.

body has different force environments, as shown in Figure 1(a) "A" and "B". Similarly, for medium and thick seam mining, this is the case with coal mining work surfaces, as shown in Figure 1(b) "C". Area "A" indicates that the coal-rock combined body within the uniaxial stress or biaxial stress state, and areas "B" and "C" represent coal-rock combined bodies within different heights under three-dimensional stress states, respectively. Therefore, the experiment revolves around the coal-rock combined body under different surrounding rock pressures and different height ratio conditions.

In the process of coal-rock combined body loading, the stress of the rock and coal body is actually consistent. The rock strength is much larger than the coal body; therefore, if the rock body has been in the elastic stage in the test process, the weak coal body is destroyed first so that the overall stress of the coal-rock combined body is reduced. Rocks, on the other hand, undergo an unloading process, and rock unloading releases a portion of the energy that exacerbates the destruction of coal. As the input source of external total energy, the test machine does some of the work on the rock specimen, part of which is converted into elastic energy stored in the rock body. After the composition test piece reaches the peak strength, with the sudden rupture failure of the block, the sudden release of accumulated energy and the rest of the dissipation energy leads to the destruction of the rock. Therefore, the rock destruction process is actually the process of state instability driven by energy.

Figure 2 shows the typical loading curve of coal-rock combination in the stress and strain coordinate system, including the prepeak loading and stress reduction stages of the rock in the coal-rock combination. The rock strength in the coal-rock combined body is greater than that of the coal body. Therefore, in the loading process, the coal body reaches the peak strength first, and then, the stress of the coal-rock combined body decreases, resulting in a stres?s reduction stage of rock in the coal-rock combined body. When the peak stress of the composition is reached, the corresponding strain of the rock part is ε_r, and the strain of the coal-rock combined body is ε_{rc}. Therefore, the energy of coal volume accumulation in the coal-rock combined body should be the difference between the total energy and the energy in the rock.

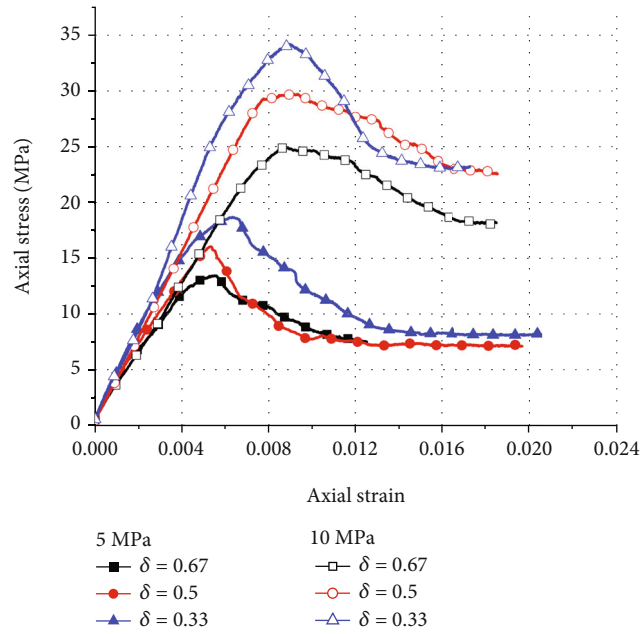

Figure 4: Stress-strain curve of coal-rock combined bodies.

The ultimate purpose of coal rock combination tests are to understand the interaction relationship between coal and rock. In order to study the energy transfer between the two blocks of the coal-rock combined body in the loading process, the experiment was divided into two parts, the standard specimen loading test and the small-size rock sample loading and unloading test.

The rock samples were taken from No. 25 Mining Area of Zhangcun Coal Mine, Shanxi Province, China. The coal-rock combined body is composed of coal and rock bodies in accordance with different height proportions in a standard specimen. The standard specimen loading test is divided into the uniaxial and conventional triaxial compression tests, which contain three sets of coal-rock combined bodies with different height ratios. δ represents the height of coal as a proportion of the height of the complete specimen, which are 0.33, 0.5, and 0.67. The conventional triaxial compression tests were conducted with six test pieces in each

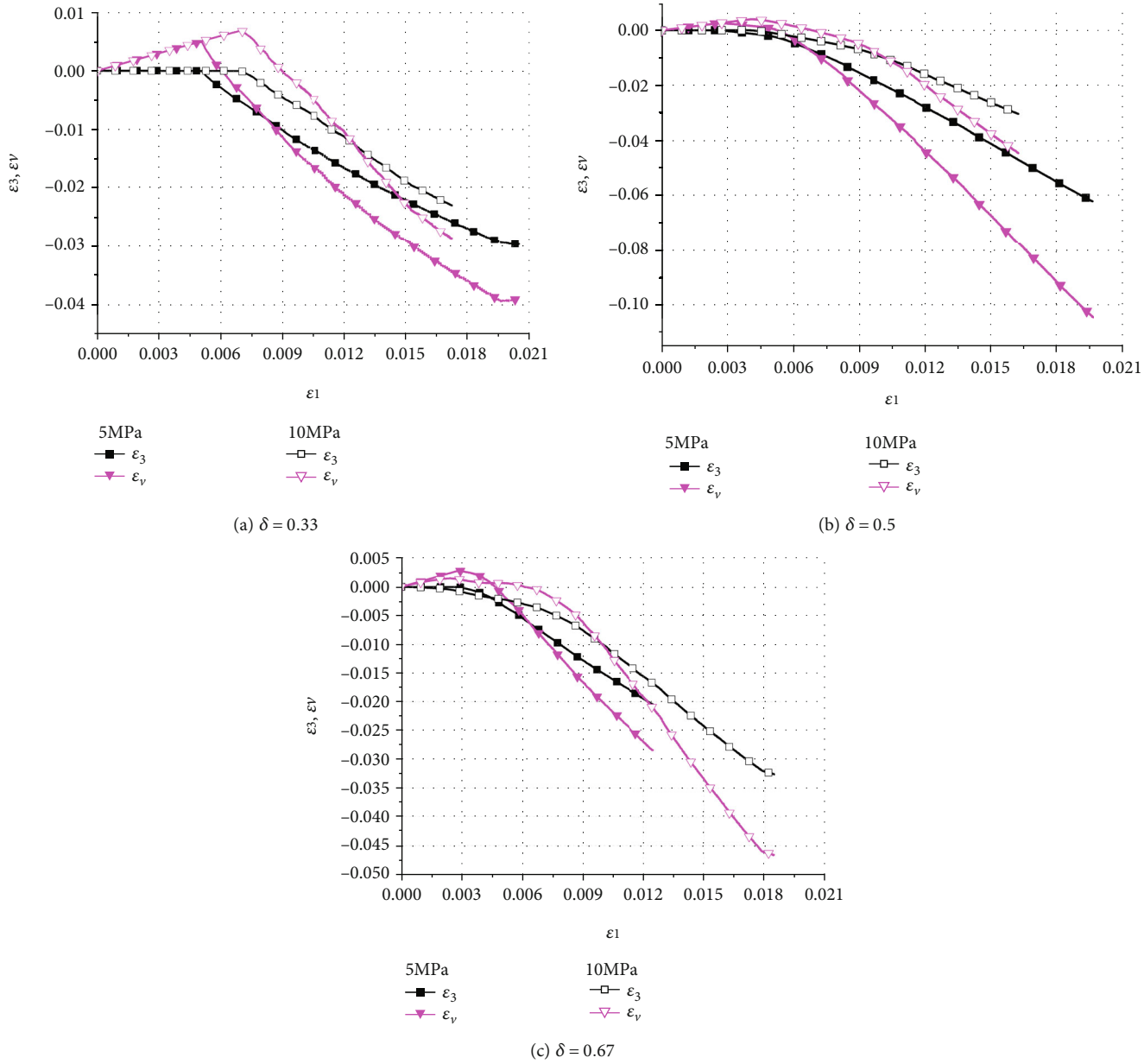

Figure 5: Relationship between lateral and volumetric strain and axial strain of coal-rock combined bodies. $\varepsilon_1, \varepsilon_3, \varepsilon_v$ represent axial strain, lateral strain, and circumferential strain, respectively.

group, with a peripressure strength of 5 MPa and 10 MPa. The test results that displayed large differences from the specimen data were removed, and the remaining groups were used to obtain the average values. The test was completed on the MTS815.02 electroliquid servo rock mechanics test equipment at China University of Mining and Technology, as shown in Figure 3.

The small-size rock sample loading and unloading tests were carried out according to the rock sample heights in the standard coal-rock combined bodies, which were 33 mm, 50 mm, and 67 mm.

Firstly, the petroleum jelly was applied to both ends of the samples; then, two layers of heat shrinkable films and ethylene-propylene self-adhesive tape were used to prevent the oil from seeping in. Secondly, installed the hoop extensometer and dropped the triaxial cell. Finally, loaded the axial pressure and used the displacement control mode until the sample was broken. In order to make the small-size rock sample reach the peak strength of coal-rock combination, the loading rate of the small rock sample was 0.5 kN/s according to the force control, which is consistent with the loading rate of the combined coal-rock body. According to the stress-strain curve, the average unloading rate of the small-sized rock sample and the postpeak unloading rate of the coal-rock combined body were consistent after failure. The loading speed was 0.003 mm/s after the cycle, and unloading was completed with displacement control, up until the point at which loading damage occurred.

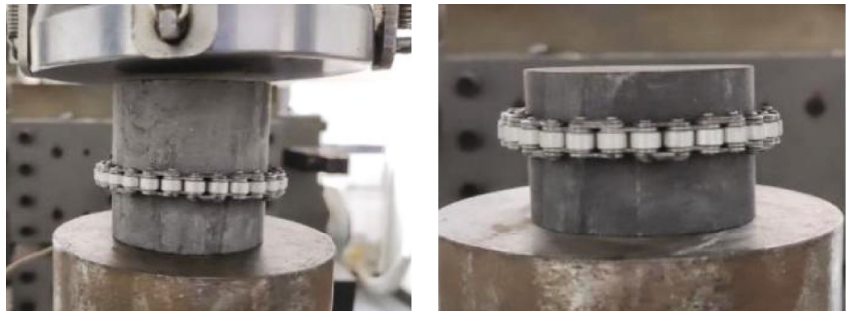

(a) Single loading and unloading tests

(b) Conventional triaxial loading and unloading mechanical tests

(c) Deformation of rock in loading and unloading tests

Figure 6: Loading and unloading tests and deformation of rocks at different heights.

3. Test Results

The stress-strain curves of the coal-rock combined bodies with different height ratios under different surrounding rock pressures are shown in Figure 4. The relationship curve between lateral, volumetric strain and axial strain are shown in Figure 5.

Conventional triaxial compression test loading preloads of 5 MPa and 10 MPa surrounding rock pressures on coal-rock combined bodies. The compaction stage of coal-rock combined bodies was not apparent, but there were clear elastic, yielding, and postpeak softening stages in both pressure cases. When $\delta = 0.33$, 0.5, and 0.67, and the surrounding rock pressure was 5 MPa, the peak strengths of coal-rock combined bodies were 17.92 MPa, 16.02 MPa, and 13.33 MPa, the elastic modulus of coal-rock combined bodies were 3.38 GPa, 3.52 GPa, and 3.58 GPa, respectively, and the axial strain varied from 0.005 to 0.00632. When the surrounding rock pressure was 10 MPa, the peak strength was 33.92 MPa, 29.51 MPa, and 24.57 MPa, the elastic modulus of coal-rock combined bodies were 3.89 GPa, 4.48 GPa, and 4.63GPa, respectively, and the axial strain varied between 0.0077 and 0.0091. As the value of δ increased, the peak stress of the coal-rock combined bodies gradually decreased, and the change trend was small. Increasing the surrounding rock pressure significantly impacted the strength of the combination, and the peak stress and post-peak residual strength values both significantly increased. The strength of the coal-rock combined bodies with different height ratios increased, and the stress drop rate after the peak also increased accordingly.

In the process of conventional triaxial compression tests, the lateral extensometer is placed on the coal body in the coal-rock combined bodies, and the measured value is the lateral strain of the coal body. The deformation and failure characteristics of the coal in the coal-rock combined bodies

can be used as the lateral strain. The relationship between volumetric strain and axial strain was obtained. As shown in Figures 5(a)–5(c), the lateral strain compression was positive, expansion was negative, volume compression was positive, and expansion was negative. With the loading of the axial force, the coal-rock combined bodies are in a compressed state. When the load is small, the coal-rock combined bodies are in the elastic stage, and the lateral strain hardly changes. As the loading progresses, the lateral strain gradually increases after reaching the peak stress. The volumetric strain of the coal-rock combined bodies showed a trend of first being positive and then negative, indicating that in the initial loading stage, the internal fissures of the coal-rock combined bodies are gradually closed, the volume is compressed, and then, new fractures are gradually formed. As the loading progresses, the cracks expand and penetrate, and the volume gradually increases and expands at an increasing rate. The ratio of the volume of the coal-rock combined bodies to the axial strain in the postpeak stage is close to the constant value, indicating that the Poisson's ratio of the coal-rock combined bodies in the postpeak stage is a constant value. With the same value of δ, the greater the surrounding rock pressure, the smaller the increasing rate of lateral and volumetric strain in the postpeak stage.

The uniaxial and conventional triaxial compression tests and loading and unloading tests of rocks with different heights are shown in Figure 6.

It can be seen in Figure 6 that the rock exhibits tensile failure when loaded under uniaxial and surrounding rock pressure. The tensile failure surface of the uniaxial test was along the axial direction of the rock, and the number of fracture stripes was larger. With the confined pressure loading, there was a gradual transition to shear failure, and the number of rupture stripes decreased.

4. Analysis and Discussion

In this section, from the energy point of view, the sample with $\delta = 0.33$ is taken as an example for illustration. The uniaxial and conventional triaxial loading and unloading mechanical tests of rock samples and cyclic loading and unloading tests of coal-rock combined bodies were carried out. The rock was loaded to the peak strength of the coal-rock combined bodies and then unloaded.

The single loading and unloading test curves for the rock are shown in Figure 7. The rest of the results are shown in Table 1.

Assuming that $f(\varepsilon)$ and $f_1(\varepsilon)$ are the loading and unloading curve functions of the rock, respectively, u_e and u_d are the elastic and dissipated strain energy densities of the rock in a single loading cycle, and u is the total input energy density, which can be expressed separately as

$$u = \int_{\varepsilon_a}^{\varepsilon_c} f(\varepsilon) d\varepsilon, \tag{1}$$

$$u_e = \int_{\varepsilon_b}^{\varepsilon_c} f_1(\varepsilon) d\varepsilon, \tag{2}$$

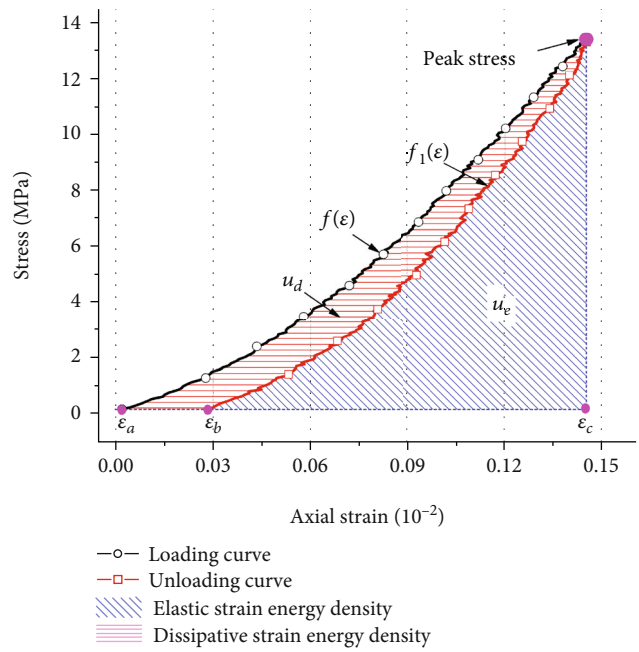

Figure 7: Single loading and unloading tests of rock.

$$u_d = u - u_e, \tag{3}$$

where ϵ_a is the initial strain of the rock, ε_b is the strain of the rock after unloading, and ε_c is the strain corresponding to the rock reaching the peak stress of the coal-rock combined body.

As the total strain energy density in the rock continues to increase with the loading process, the total strain energy density is always larger than the elastic strain energy density, and when the load reaches the peak strength of coal rock combination, the unloading process begins. At the unloading point, the maximum total strain energy density is 7.89 KJ/m^3, and the energy is dissipated during unloading. When unloading to the initial stress value, the dissipation strain energy density reaches the maximum value of 1.7 KJ/m^3, and the elastic strain energy density reaches the maximum value of 5.43 KJ/m^3. In the initial stage, the rock consumes energy due to the closure of cracks or internal voids. At this time, u_d is slightly higher than u_e, but the increase in u_e is much larger than u_d. The difference between u and u_e continues to increase, that is, the density of the dissipated strain energy continues to increase, and the increasing trend is relatively slow.

Under different surrounding rock pressures, unloading process begins when the rock is loaded to the peak strength of the combined sample. The strain energy density obtained by the test is shown in Table 1. It can be seen that the total strain energy density of the rock increases with the increase in the surrounding rock pressure, while the elastic strain energy density and the dissipated strain energy density also increase. The dissipated energy in the rock is mainly caused by the unloading deformation and rebound of the rock. This part of the energy plays a role in the secondary loading of the coal during the loading process of the coal-rock combined bodies. The greater the surrounding rock pressure, the greater the rebound energy of the rock.

Table 1: Rock strain energy density.

δ	Surrounding rock pressure/MPa	Maximum loading stress/MPa	Total strain energy density/KJ·m^{-3}	Elastic strain energy density/KJ·m^{-3}	Dissipated strain energy density/KJ·m^{-3}	Percentage of dissipated energy
0.33	0	6.5	4.302	3.74	0.562	13.06%
	5	12	7.899	6.013	1.886	23.8%
	10	25	26.023	14.889	11.134	42.7%

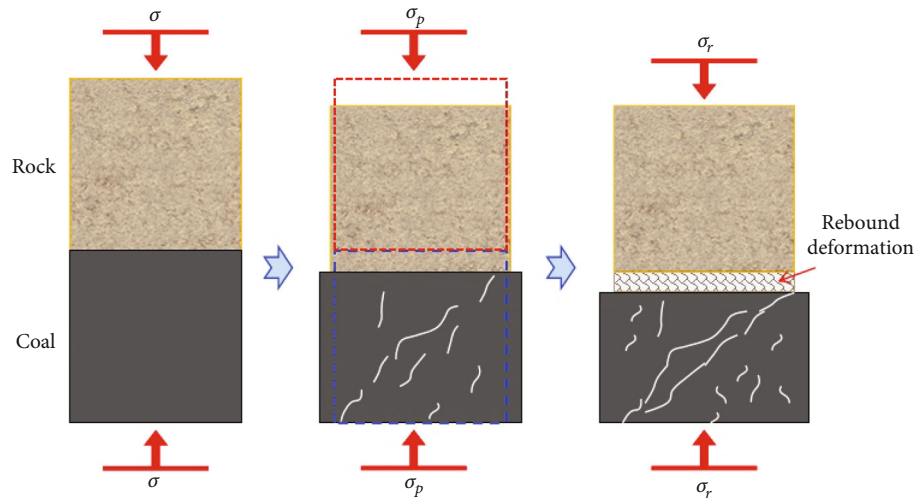

Figure 8: Coal-rock combined body deformation and rock rebound deformation process.

During the loading process of coal-rock combined bodies, the maximum strength value of rock is equal to the peak strength value of coal-rock combined bodies. After that, when the coal-rock combination reaches the post peak stage, the strength of rock will not increase, and it will remain consistent with the residual strength of the combination until it reaches the residual strength. During the unloading process, because the rock is in the elastic stage, the deformation rebounds, and the rebound deformation performs secondary loading to the coal body, which accelerates the failure and destruction of the coal body. The rebound effect of the rock during the deformation process is shown in Figure 8.

The relationship between the total energy of the coal-rock combined bodies in the prepeak stage and the total energy stored in the coal and rock masses is shown in

$$U_{rc} = U_c + U_r, \tag{4}$$

where U_{rc} is the total energy stored in the coal-rock combined bodies, U_c is the energy stored inside the coal body, and U_r is the energy stored inside the rock damage.

According to the test results, the energy accumulation of each monomer in the coal-rock combined bodies can be obtained, as shown in Table 2.

In the coal–rock combined bodies, due to the high rock strength and small deformation, the confining pressure and initial loading slow down the crack closure, so the stress–strain curve of the rock crack closure stage is more concave, which is not conducive to the energy accumulation in the rock. The energy accumulation inside the coal body in the coal-rock combined bodies shows an increasing trend according to the increase in the proportion of the coal body, and the energy proportion is between 60% and 85%. The relatively weak coal in the coal-rock combined bodies is the main energy carrier. This is because the peak elastic energy density is not only affected by the peak strength but also related to the peak strain. During the loading process of coal-rock combined bodies, the stress values of coal and rock mass are equal, but the peak strain of coal is much greater than that of the rock mass. According to the stress-strain relationship of coal and rock in Figures 4 and 7, when the surrounding rock pressure is 5 MPa, the rock mass strain accounts for about 26.1% of the peak strain of the coal-rock combined bodies. Meanwhile, the strain produced by pure rock is far less than that of the coal in coal-rock combined bodies, resulting in low peak elastic energy density and low stored elastic energy of rock specimens.

In order to reveal the relationship between the overall energy transfer of coal-rock combined bodies and the energy transfer of coal and rock, under the surrounding rock pressure of 5 MPa, $\delta = 0.67$, the energy evolution of coal-rock combined bodies under cyclic loading and unloading is selected as an example.

The cyclic loading and unloading curves of coal-rock combined bodies are shown in Figure 9. There are six cycles in total. The loading and unloading rates are consistent with that of small-sized rock samples, and the last loading occurs until failure. Figure 10 shows the relationship curve between internal energy and axial stress of coal-rock combined bodies.

In the cyclic loading and unloading process, the total input energy density u, elastic strain energy density u_e and dissipated strain energy density u_d of coal-rock combined

Table 2: Strain energy density of combinations and monomers.

δ	Surrounding rock pressure/MPa	Strain energy density/KJ·m^{-3}			Coal energy ratio
		Coal-rock combined bodies	Coal	Rock	
0.67	0	15.7	11.4	4.3	72.7%
	5	45.82	37.92	7.899	82.8%
	10	122.4	96.38	26.02	78.8%
0.5	0	19.3	11.88	7.411	61.6%
	5	47.5	32.82	14.675	69.2%
	10	155.9	97.28	58.62	62.4%

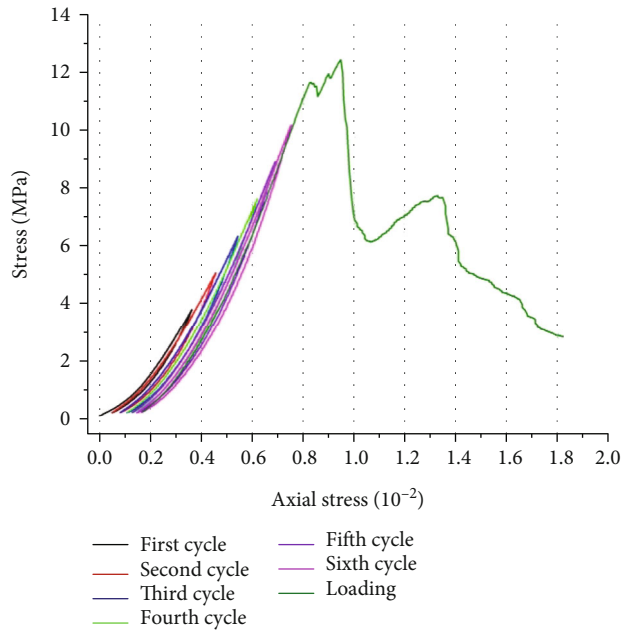

Figure 9: Cyclic loading and unloading of coal-rock combined bodies.

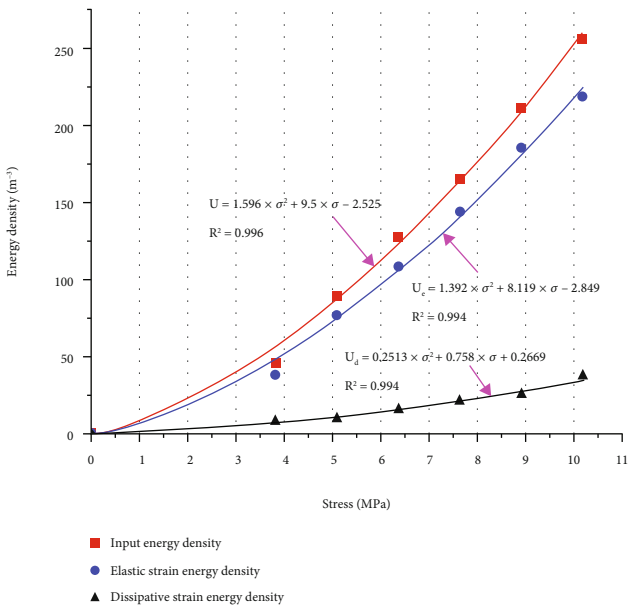

Figure 10: Evolution law of energy and axial stress of coal-rock combined bodies.

bodies increase with the increase in axial stress σ. These all show the same nonlinear correlation with axial stress σ and a quadratic polynomial can express its functional relationship, as shown in Figure 10. The relationship between total input energy density, elastic strain energy density, dissipated strain energy density, and axial stress of coal-rock combined bodies can be divided into three stages: (1) energy stable stage. When the axial stress is less than 5 MPa, the internal primary microcracks and defects of the coal-rock combined bodies are gradually closed under the action of the external load. The difference between the elastic strain and the input energy density curves is very small, indicating that the input energy at this stage is mainly stored in the coal-rock combined bodies in the form of elastic strain energy. In contrast, less-dissipated strain energy is used for primary cracks, defect propagation, and new crack generation. (2) Rapid energy accumulation stage. When the axial stress increases from 5 MPa to 9 MPa, the coal-rock combined bodies show that the elastic energy evolution curve increases greatly compared with the previous stage. The input energy and elastic strain energy of coal-rock combined bodies increase rapidly, and the increment of dissipated energy is still small. The coal-rock combined bodies are mainly stored elastic energy. (3) Rapid energy dissipation stage. When the axial stress increases from 9 MPa to about 10.5 MPa, the dissipated strain energy "suddenly increases," and the coal-rock combined bodies begin to enter the stage of unstable fracture development, indicating that the coal-rock combined bodies produce unrecoverable deformation at this stage, and the internal cracks expand and penetrate and gradually form macrocracks.

The input energy, elastic strain energy, and dissipated strain energy in the loading process of coal-rock combined bodies show a nonlinear growth trend. In the early stage of loading, the growth rate of input energy density, elastic energy density, and dissipated energy density is slow, which matches the compaction stage of coal and rock mass deformation. This shows that a small part of the energy in the evolution process is used for dissipation, and the rest of the energy is transformed into elastic properties. Then, in the stage of elastic deformation, a large amount of energy is accumulated. Finally, with the "sudden increase" in dissipated energy, the coal-rock combined bodies begin to enter the stage of unstable fracture development. In coal-rock combined bodies, the coal body is the main carrier of energy, accounting for more than 60%, and the energy accumulation

Figure 11: Crack propagation during loading of the coal-rock combined body.

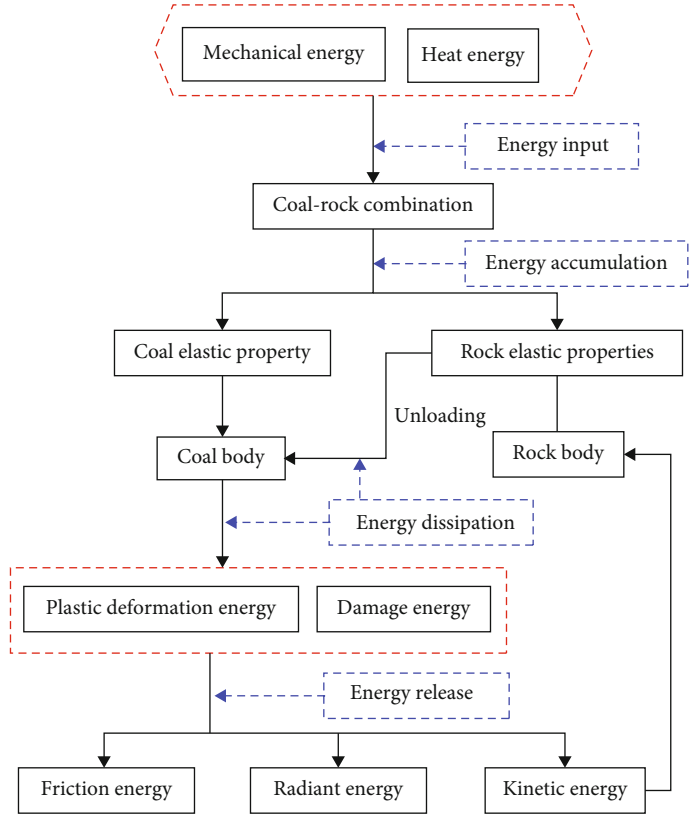

Figure 12: Schematic diagram of energy transfer.

shows an increasing trend with the increase in the proportion of the coal body. The failure of the coal-rock assemblage is mainly due to the failure of the coal body. After reaching the yield load, most of the energy in the coal body is dissipated in the form of plastic deformation and internal damage of the coal body and is released in the form of block friction, radiation energy, and kinetic energy when the crack penetrates. Part of the released energy reacts to the rock mass, and cracks appear in the rock mass, as shown in Figure 11. After the stress in the coal mass is reduced, the elastic deformation energy in the rock mass is released, acting on the coal mass and aggravating the plastic deformation and damage of the coal mass. The energy transfer between the two is shown in Figure 12.

Crack propagation sketches of three different coal-rock combined bodies when the surrounding rock pressure is 5 MPa as shown in Figure 12. It can be seen that the coal body part of the coal-rock combined bodies is more severely fractured, and there are apparent shear fracture zones, indicating that the coal body is in shear failure. The slip dislocation of the upper and lower blocks of the shear zone is the main reason for the increase in the lateral deformation of the coal-rock combined bodies in the postpeak stage. There are obvious cracks in the rock part of the coal-rock combined bodies, most of which are the tensile failure of a single crack. The angle between the crack and the vertical direction is small, close to vertical, and the starting position is close to the fracture zone in the coal body. Since the strength of the coal body in the coal-rock combined bodies is much smaller than the rock body when the coal body is destroyed, the rock body is in the prepeak stage. The occurrence of cracks in the rock is mainly due to the energy released when the coal body is destroyed, which is partially converted into kinetic energy, which reacts in the rock body and causes cracks.

5. Conclusion

In this study, a single rock sample with the same size as the rock sample in the coal-rock combination is used to simulate the loading and stress reduction process in the loading process of the coal-rock combination. The characteristics of energy transfer in coal-rock combined bodies are clarified through the compression tests. The main conclusions of this study are as follows:

(1) As the value of δ (height proportion of coal in coal rock combined bodies) increases, the peak stress of the coal-rock combined bodies gradually decreases, increasing the pressure of the surrounding rock, which has a significant impact on the strength of the assembly and both the peak stress and postpeak residual strength value increase significantly. With the same value of δ, the greater the surrounding rock pressure, the smaller the increasing rate of lateral and volumetric strain in the postpeak stage

(2) In the initial loading, the coal-rock combined body is compressed first, the internal fissures in the rock are gradually closed, and the volume is reduced. As the loading progresses, new cracks are gradually formed, the cracks expand and penetrate, and the volume gradually increases and expands at an increasing rate

(3) The energy accumulation and dissipation of coal rock assemblage can be divided into the following stages: energy stable stage, rapid energy accumulation stage, and rapid energy dissipation stage. The change in energy accumulation and dissipation shows a nonlinear growth trend. The energy is dissipated when unloading, and part of the dissipated energy in the rock acts as a secondary load on the coal body. At the same time, when the coal body fails, the energy is released and converted into kinetic energy, causing the rock body to show tension and failure due to a single fracture

(4) The energy accumulation inside the coal body in the coal-rock combined bodies shows an increasing trend according to the increase in the proportion of the coal body. When δ is between 0.5 and 0.67, the proportion of coal energy is between 60% and 85%, respectively, under different surrounding rock pressures

(5) The peak strain of coal is much greater than that of the rock mass, and the stress values of coal and rock mass are equal, resulting in the relatively weak coal body in the coal-rock assembly being the main carrier of energy

Data Availability

The (data type) data used to support the findings of this study are included within the article.

Conflicts of Interest

The authors declare no conflicts of interest.

Authors' Contributions

Tuo Wang and Jucai Chang conceived and established the experimental system. Tuo Wang wrote the paper.

Acknowledgments

This research was funded by the University Natural Science Research Project of Anhui Province (KJ2021A0453), the Talent Introduction Research Start-Up Fund of Anhui University of Science and Technology (13210673), the National Natural Science Foundation of China (grant numbers 51774009 and 52174105), the Anhui Province Key Research and Development Program Funded Project (202004a07020045), and the Anhui Province University Collaborative Innovation Project (GXXT-2019-029).

References

[1] Z. Yubao, *Research on the Failure Mechanism of Road Ledge Based on Rock Crack Damage Effect*, Shandong University of Science and Technology, 2019.

[2] H. Xie, J. Zhu, T. Zhou, and J. Zhao, "Novel three-dimensional rock dynamic tests using the true triaxial electromagnetic Hopkinson bar system," *Rock Mechanics and Rock Engineering*, vol. 54, no. 4, pp. 2079–2086, 2021.

[3] O. Rodriguez-Villarreal, A. Varela Valdez, C. La Borderie, G. Pijaudier-Cabot, and M. Hinojosa Rivera, "Estimation of fracture energy from hydraulic fracture tests on mortar and rocks at geothermal reservoir temperatures," *Rock Mechanics and Rock Engineering*, vol. 54, no. 8, pp. 4111–4119, 2021.

[4] Z. Liming, G. Gao, R. Mingyuan, W. Zaiquan, and M. Shaoqiong, "Evolution characteristics of elastic energy and dissipated energy of rock failure under load," *Journal of China Coal Society*, vol. 39, no. 7, pp. 1238–1242, 2014.

[5] Z. Zhizhen and G. Feng, "Study on the nonlinear characteristics of rock energy evolution under uniaxial compression," *Chinese Journal of Rock Mechanics and Engineering*, vol. 31, no. 6, pp. 1198–1207, 2012.

[6] Z. Minghua, L. Sisi, H. Lixiong, and L. Binbin, "Numerical simulation calculation of pressure anchor based on energy principle," *Chinese Journal of Geotechnical Engineering.*, vol. 4, pp. 529–534, 2011.

[7] P. Hou, Y. Xue, F. Gao et al., "Effect of liquid nitrogen cooling on mechanical characteristics and fracture morphology of layer coal under Brazilian splitting test," *International Journal of Rock Mechanics and Mining Sciences*, vol. 151, p. 105026, 2022.

[8] Y. Xue, J. Liu, P. G. Ranjith, Z. Zhang, F. Gao, and S. Wang, "Experimental investigation on the nonlinear characteristics of energy evolution and failure characteristics of coal under different gas pressures," *Bulletin of Engineering Geology and the Environment*, vol. 81, no. 1, pp. 1–26, 2022.

[9] L. M. Vasil'Ev and D. L. Vasil'Ev, "Contact friction included in the problem on rock failure under compression," *Journal of Mining Science*, vol. 51, no. 3, pp. 462–469, 2015.

[10] A. D. Alexeev, V. N. Revva, L. L. Bachurin, and I. Y. Prokhorov, "The effect of stress state factor on fracture of sandstones under true triaxial loading," *International Journal of Fracture*, vol. 149, no. 1, pp. 1–10, 2008.

[11] N. Cook, *The Design Of Underground Excavations*, American Rock Mechanics Association, 1966.

[12] L. Gao, F. Gao, Y. Xing, and Z. Zhang, "An energy preservation index for evaluating the rockburst potential based on energy evolution," *Based on Energy Evolution*, vol. 13, no. 14, pp. 3636–3651, 2020.

[13] F. Gong, J. Yan, X. Li, and S. Luo, "A peak-strength strain energy storage index for rock burst proneness of rock materials," *International Journal of Rock Mechanics and Mining Sciences (Oxford, England : 2019)*, vol. 117, pp. 76–89, 2019.

[14] F. Gong, Y. Wang, Z. Wang, J. Pan, and S. Luo, "A new criterion of coal burst proneness based on the residual elastic energy index," *International Journal of Mining Science and Technology*, vol. 31, no. 4, pp. 553–563, 2021.

[15] Q. B. Meng, C. K. Wang, B. X. Huang et al., "Rock energy evolution and distribution law under triaxial cyclic loading and unloading conditions," *Chinese Journal of Rock Mechanics and Engineering*, vol. 39, no. 10, pp. 2047–2059, 2020.

[16] Q. Tu, Y. Cheng, S. Xue, T. Ren, and X. Cheng, "Energy-limiting factor for coal and gas outburst occurrence in intact coal seam," *International Journal of Mining Science and Technology*, vol. 31, no. 4, pp. 729–742, 2021.

[17] M. He, Z. Zhang, J. Zhu, and N. Li, "Correlation between the constant mi of Hoek–Brown criterion and porosity of intact rock," *Rock Mechanics and Rock Engineering*, vol. 55, no. 2, pp. 923–936, 2022.

[18] B. Yang, M. He, Z. Zhang, J. Zhu, and Y. Chen, "A new criterion of strain rockburst in consideration of the plastic zone of tunnel surrounding rock," *Rock Mechanics and Rock Engineering*, vol. 55, no. 3, pp. 1777–1789, 2022.

[19] Y. Erhao, *Experimental Study on Uniaxial Compression Acoustic Emission Characteristics and Crack Propagation Law of Coal-Rock Combined Bodie*, Xi'an University of Science and Technology, 2019.

[20] C. Shaojie, Y. Dawei, Z. Baoliang, M. Hongfa, and L. Xingquan, "Study on the mechanical properties of roof-coal pillar structure and its progressive failure mechanism," *Chinese Journal of Rock Mechanics and Engineering*, vol. 36, no. 7, pp. 1588–1598, 2017.

[21] W. Ning, *Research on the Disaster Mechanism and Prevention of Rock Burst under the Combination of Hard Coal and Rock*, China University of Mining and Technology (Beijing), 2015.

[22] L. Peng, T. Chunan, C. Zhonghui, and H. Runqiu, "Numerical simulation and experimental study on the whole failure process of the two rock mass system," *Earth*, vol. 19, no. 4, pp. 413–418, 1999.

[23] G. Huali, *Experimental Study on Mechanical Failure of Gas-Containing Coal Seam Assembly and Its Energy Evolution Experiment*, China Coal Research Institute, 2020.

[24] H. Wang, C. Jiang, P. Zheng, W. Zhao, and N. Li, "A combined supporting system based on filled-wall method for semi coal-rock roadways with large deformations," *Tunnelling and Underground Space Technology*, vol. 99, p. 103382, 2020.

[25] L. Fujun, Y. Zuncai, B. Maiying, Q. Hengchang, D. Tingbin, and Y. Dawei, "Review of research on the stability of roof-coal pillar combination," *Coal Mine Safety.*, vol. 50, no. 8, pp. 209–212, 2019.

[26] Q. Xiao, *Experimental Study on the Influence of Roof and Floor Mechanical Properties on the Stability of Strip Coal Pillars*, Shandong University of Science and Technology, 2018.

[27] W. Hui, *The Mechanism and Application of Composite Weak Structure to Prevent and Control Rock Burst*, Shandong University of Science and Technology, 2017.

[28] G. Chen, T. Li, G. Zhang, P. Teng, and B. Gong, "Energy distribution law of dynamic failure of coal-rock combined body," *Rock and Soil Mechanics*, vol. 2021, article 6695935, 14 pages, 2021.

[29] L. Chengjie, X. Ying, F. Mingming, and P. Bin, "Deformation law and failure mechanism of coal-like rock combination under uniaxial load," *Journal of China Coal Society*, vol. 45, no. 5, pp. 1773–1782, 2020.

[30] Y. Weijian, W. Genshui, L. Ze, L. Yi, H. Zhong, and L. Fangfang, "Experimental study on uneven failure of loose coal-rock combined bodies," *Coal Science and Technology.*, vol. 47, no. 1, pp. 85–90, 2019.

[31] C. Yan, Z. Jianping, S. Hongqiang, F. Lulu, and S. Guangyao, "Research on cyclic loading and unloading deformation and crack evolution law of coal-rock combined bodies," *Journal of Mining & Safety Engineering.*, vol. 35, no. 4, pp. 826–833, 2018.

[32] J. P. Zuo, H. Q. Song, Y. Chen, and Y. H. Li, "Post-peak progressive failure characteristics and nonlinear model of coal-rock combined bodies," *Journal of China Coal Society*, vol. 43, no. 12, pp. 3265–3272, 2018.

[33] X. Xiaochun, F. Yufeng, and W. Di, "Research on the relationship between combined coal and rock mechanical properties and acoustic_charge signal_Xiao Xiaochun," *China Work Safety Science and Technology.*, vol. 14, no. 2, pp. 126–132, 2018.

[34] D. Linming, T. Jingcheng, L. Caiping et al., "Study on electromagnetic radiation law of combined coal and rock impact failure," *Chinese Journal of Rock Mechanics and Engineering*, vol. 19, pp. 143–146, 2005.

[35] X. S. Liu, J. G. Ning, Y. L. Tan, and Q. H. Gu, "Damage constitutive model based on energy dissipation for intact rock subjected to cyclic loading," *International Journal of Rock Mechanics and Mining Sciences*, vol. 85, pp. 27–32, 2016.

[36] Z. Huan, *Research on the Effect of Local Impact on Coal and Rock Microstructure and Equivalent Theoretical Model*, China University of Mining and Technology (Beijing), 2019.

[37] C. Zhiyun, *Research on Constitutive Model of Creep Damage of Coal and Rock around Borehole for Water-Bearing Gas Drainage*, Xi'an University of Science and Technology, 2020.

[38] C. Guangbo, Z. Junwen, L. Tan et al., "Study on the time-effect of damage and deterioration of mechanical properties of coal-rock combined bodies under the action of water and rock," *Journal of China Coal Society*, pp. 1–18, 2021.

[39] L. Bobo, W. Zhonghui, R. Chonghong, Z. Yao, X. Jiang, and L. Jianhua, "Study on coal and rock mechanical properties and damage constitutive model under hydraulic-mechanical coupling," *Rock and Soil Mechanics*, vol. 42, no. 2, pp. 315–323, 2021.

[40] X. Lin, F. Mingze, X. Jun et al., "Development and application of one-way heating simulation test device for coal and rock," *Journal of China Coal Society*, vol. 46, no. 6, pp. 1738–1746, 2021.